

Feature Article

“Smart” nanoparticles: Preparation, characterization and applications

Matthias Ballauff, Yan Lu*

Physikalische Chemie I, University of Bayreuth, 95440 Bayreuth, Germany

Received 27 October 2006; received in revised form 1 February 2007; accepted 2 February 2007

Available online 7 February 2007

Abstract

We review recent work on the preparation, characterization and application of “smart” microgel particles. A general feature of all systems under consideration here is their ability to react to external stimuli as e.g. the pH or the temperature in the system. Special emphasis is laid on our recent research work on the thermosensitive core–shell microgel particles, which are composed of a PS core and a cross-linked poly(*N*-isopropylacrylamide) (PNIPA) shell. Work done on these core–shell systems is compared to developments on the investigations of similar systems. A novel synthesis method, namely photo-emulsion polymerization, has been described for the preparation of monodisperse, thermosensitive core–shell particles. Cryogenic transmission electron microscopy (cryo-TEM) has recently been employed to investigate the morphology and the volume transition of the core–shell type microgels. This method furnishes information about the thermosensitive particles that had not been available through other methods employed in previous investigations. Very recently, it has been shown that these core–shell microgels can be used as “nanoreactors” for the immobilization of metal nanoparticles. The metal nanocomposite particles show “smart” catalytic behaviour, inasmuch as the catalytic activity of nanoparticles can be switched on and off through the volume transition that takes place within the thermosensitive shell of the carrier system. We also discuss possible future applications of these systems.

© 2007 Elsevier Ltd. All rights reserved.

Keywords: Microgels; Thermosensitive; Core–shell

1. Introduction

Environmentally responsive microgels have been subjects of great interest in the last two decades due to their versatile application [1]. Such microgels are sometimes termed “smart” since their properties allow them to react in a specific way to external stimuli. Hence, such “smart” materials can be made responsive to various parameters, such as temperature [2,3], pH [4,5], light [6], ionic strength [7], and magnetic fields [8]. Applications of these systems range from various fields like drug delivery [9–11], biosensing [12], chemical separation [13], biomaterials [14,15] and catalysis [16–20].

Most of these systems are based on poly(*N*-isopropylacrylamide) (PNIPA) or related copolymers [1,2]. In aqueous media, PNIPA exhibits a lower critical solution temperature

(LCST) at about 32 °C, which is close to the physiological temperature [21–27]. Below the LCST, the polymer chains are soluble in water due to the formation of hydrogen bonds between the water molecules and the amide side chains. When the temperature increases, the polymer undergoes a volume phase transition. Water is expelled from the microgel interior, thus causing a drastic decrease in volume above the LCST of the polymer.

In 1986, Pelton and Chibante [28] first reported the preparation and characterization of temperature-sensitive microgels based on PNIPA. By using precipitation polymerization, homogeneous microgels with remarkably uniform morphology can be produced. Similar procedures have been described by many other research groups [29–32]. Meanwhile, core–shell type microgels, which contain a hydrophobic core and a hydrophilic thermosensitive shell, have become attractive for scientists since such systems may combine the properties characteristic of both the core and the shell [33,34]. In this case, the ends of the cross-linked PNIPA chains are fixed to

* Corresponding author.

E-mail address: yan.lu@uni-bayreuth.de (Y. Lu).

a solid core, which defines a solid boundary of the network. In this respect such core–shell latex particles present cross-linked polymer brushes onto defined spherical surfaces. The solvent quality may be changed from good solvent conditions at room temperature to poor solvent conditions at a temperature above 32 °C (see Fig. 1) [35,36]. Recently, Lyon et al. [37] have reported the preparation of core–shell particles with a degradable core. Thus, hollow thermosensitive microgels can be obtained by oxidation of the particle core, followed by removal of the produced polymer segments. Richtering et al. [38,39] have synthesized multi-responsive core–shell microgels, in which two polymers with different temperature sensitivities are combined in a spherical core–shell morphology.

When PNIPA-based microgels are functionalized with pH-ionizable, hydrophilic and reactive carboxylic acid groups, the “smart” microgels can be tuned specifically in order to generate fast and targeted swelling responses to multiple external stimuli, such as both temperature and pH [40–43]. For example, Zhou and Chu [44] have synthesized lightly cross-linked, monodisperse and submicron-sized poly(methacrylic acid-*co*-*N*-isopropylacrylamide) (PMAA-*co*-PNIPA) microgel particles in water by dispersion polymerization. They found that the coupling of pH and temperature could induce a hydrodynamic volume change as large as 10 to 100-fold of the collapsed microgel particles by adjusting the PMAA content. Li et al. [45] have developed a new method to prepare smart microgels that consist of well-defined temperature-sensitive cores with a pH-sensitive shell. The microgels were obtained from aqueous graft copolymerization of *N*-isopropylacrylamide and *N,N'*-methylenebisacrylamide from water-soluble polymers containing amino groups such as poly(ethyleneimine) and chitosan. The unique core–shell nanostructures exhibited tuneable responses to pH and temperature [45].

Here we review our recent work on core–shell type thermosensitive microgels and compare this work to decisive developments in this field. The synthesis of these core–shell microgels by conventional emulsion polymerization will be discussed and compared to the novel method of photo-emulsion polymerization. Furthermore, we demonstrate that cryogenic transmission electron microscopy (cryo-TEM, Refs. [46,47]) is the method of choice to study the morphology

of microgels in situ. Cryo-TEM has been employed to investigate the morphology and the volume transition of the core–shell type microgels during our study. Moreover, an overview of the application of such microgels as “nanoreactors” for the immobilization of metal nanoparticles is given. The metal nanocomposite particles thus obtained exhibit “smart” catalytic behaviour as the catalytic activity of nanoparticles can be modulated by a thermodynamic transition taken place within the carrier system. A final point to be addressed here is flow behaviour of concentrated suspensions of these “smart” particles. Here we discuss possible applications of this particular feature of the core–shell systems. A brief conclusion will sum up this review.

2. Synthesis of core–shell type thermosensitive microgels

Thermosensitive core–shell particles were first synthesized by Makino et al. [48], Okubo and Ahmad [49], and by us [50,51] with a two-stage approach. These particles consist of a poly(styrene) core onto which a shell of poly(*N*-isopropylacrylamide) (PS–PNIPA) has been affixed in a seeded emulsion polymerization. Pichot et al. [52,53] and Martinho et al. [54] have synthesized monodisperse core–shell particles, which consist of a core of poly(methyl methacrylate) (PMMA) and a thermosensitive shell of poly(*N*-isopropylacrylamide) (PNIPA). Recently, Xiao et al. [55] synthesized poly(acrylamide-*co*-styrene)-poly(acrylamide-acrylic acid) particles whose shells swell when the temperature increases. The thermal behaviour of these particles is opposite to the particles bearing a PNIPA shell, which will bring the opportunity for new applications.

Typically, the synthesis of core–shell type microgel particles is performed in two steps [51]. At first, the PS-seed latex is made by emulsion polymerization. A small amount of the monomer NIPA (5 wt%) is copolymerized in this step, which creates a thin shell of PNIPA onto the core particles. This hydrophilic PNIPA layer helps to stabilize the particles above the volume transition where the steric stabilization by the polymer chains of the shell is not fully operative anymore [51]. Then the PNIPA network is affixed to the PS cores by a second seeded emulsion polymerization, which is carried out at $T > LCST$. Most probably, the PNIPA network is connected to the core particles by chain transfer in this step. As water is a poor solvent for PNIPA above the LCST, the shell is obtained in the shrunken state. The suspension of core–shell particles, however, remains stable even at temperatures above the volume transition, which is due to the residual surface charge originating from the first emulsion polymerization [51].

Cryo-TEM allows a direct investigation of the particle morphology in situ [46,47,56], no staining is necessary. Recently, we published a study of core–shell microgel particles by cryogenic transmission electron microscopy (cryo-TEM) [57]. Fig. 2 shows the cryo-TEM image of the microgel particles. The thermosensitive shell can be clearly seen in this image, which shows a corona around the spherical PS core. It is worth noting that a slight irregular shape of the shell can be

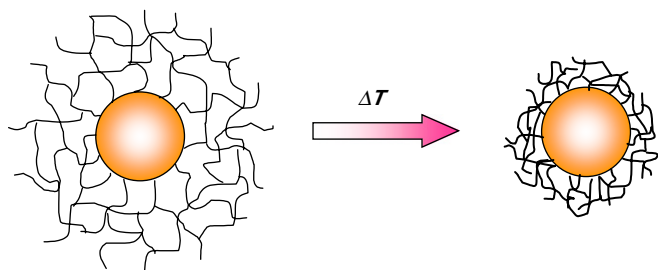


Fig. 1. Schematic representation of the volume transition in thermosensitive core–shell particles. The thermosensitive PNIPA networks are affixed to the surface of the core particles, which thus provides one boundary of the network. The solvent, water, is taken up by the network at low temperature, but it is expelled when the shell undergoes a volume transition at 32 °C.

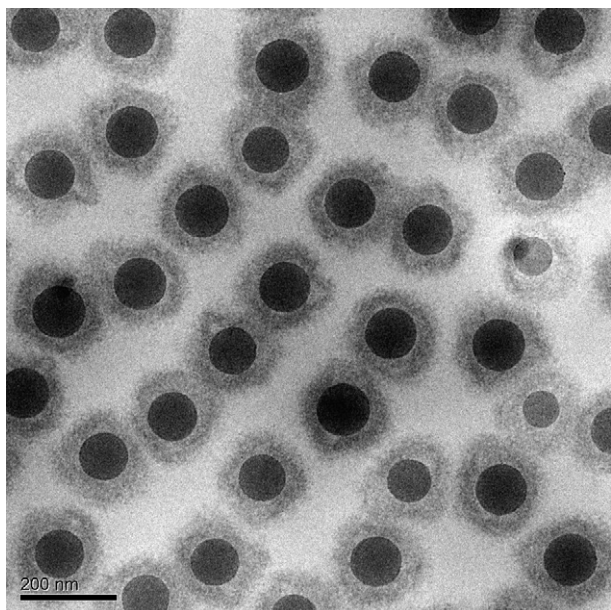


Fig. 2. Cryo-TEM image of PS–PNIPA core–shell particles. The sample was kept at 23 °C before vitrification (Ref. [57]).

observed, which is due to the density fluctuations within the network. Moreover, the inhomogeneities of the network shown in the cryo-TEM image corroborate previous finding using small-angle X-ray scattering (SAXS) [51,58]. As discussed in Ref. [51], these inhomogeneities are due to the thermal fluctuations of the polymer chains which are frozen in by the process of cross-linking. Furthermore the fact that the

cross-linker *N,N'*-methylenebisacrylamide (BIS) is consumed more rapidly than NIPA [59] may add to this as well.

The analysis of the micrographs showed an interesting new detail, which was not obvious from previous investigations: the conventional two-step process may lead to defects in which the shells may not be “stitched” onto the cores. Fig. 2 demonstrates that the shell is buckling up for some particles. This demonstrated that during the two-step process the chain transfer does not lead to complete attachment of the shell to the cores and the strong swelling of the shell at room temperature may lead to a partial detachment of the shells [57].

Photochemical initiation presents a solution to this problem. UV irradiation has been used by Kuckling et al. [60,61] as a method to synthesize thermosensitive nanogels in a well-defined fashion. Recently, Yao et al. [62] prepared poly(*N*-isopropylacrylamide) nanogels with diameters of 50–200 nm from *N*-isopropylacrylamide by photo-polymerization in the absence of initiator, cross-linker and surfactant. More recently, we employed photo-emulsion polymerization to prepare well-defined PS–PNIPA core–shell particles [63]. Some time ago, we have demonstrated that photo-emulsion polymerization can be used to affix linear polymer chains to colloidal core particles [64]. This “grafting-from” method, where the polymer layers are formed by in situ polymerization initiated by the immobilized initiators on the surface, has been employed to generate dense layers of anionic and cationic polyelectrolyte chains on PS cores in order to obtain spherical polyelectrolyte brushes [64–67]. As shown in Fig. 3, the synthesis is carried out in three steps. First the PS core particles

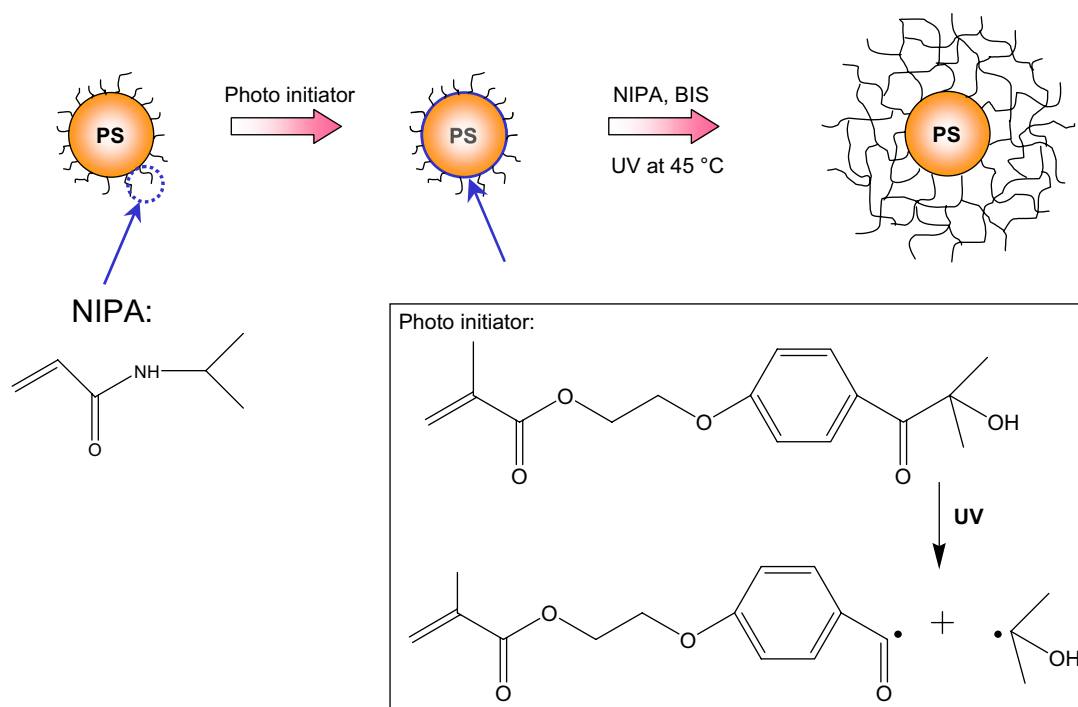


Fig. 3. Schematic representation of the preparation of PS–PNIPA core–shell particles by photo-emulsion polymerization. In the first step, a PS core with 5 mol% NIPA is prepared by emulsion polymerization. In the second step, the PS core is covered with a thin layer of photo-initiator HMEM. In the third step, the shell of cross-linked PNIPA network is formed by photo-emulsion polymerization (Ref. [63]).

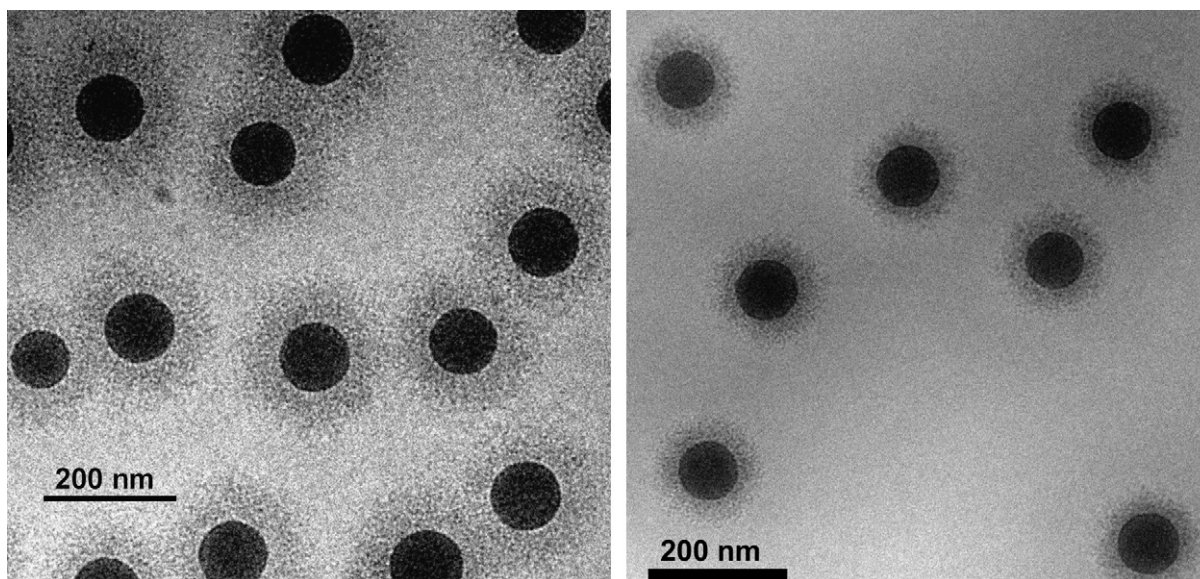


Fig. 4. Cryo-TEM images of PS–PNIPa core–shell particles prepared by photo-emulsion polymerization with different cross-linker contents: 2.5 mol% BIS (left) and 10 mol% BIS (right) (Ref. [63]).

containing 5 mol% NIPa are synthesized by a conventional emulsion polymerization. Then these core particles are covered by a thin layer of the photo-initiator 2-[*p*-(2-hydroxy-2-methylpropiophenone)]-ethyleneglycol methacrylate (HMEM) which is also a monomer. This is achieved by slow addition of HMEM after 1 h reaction of the first step when the styrene has not been fully converted to solid PS, namely under “starved condition”. In the third step, the photo-emulsion polymerization is carried out by shining light onto a suspension of these particles thereby generating radicals on their surface. The polymerization is initiated by these radicals and cross-linked PNIPa chains are generated by this grafting-from method by using *N,N'*-methylenebisacrylamide (BIS) as the cross-linker. Fig. 4 displays the cryo-TEM images of PS–PNIPa core–shell particles prepared by photo-emulsion polymerization. The cryo-TEM images indicate clearly the core–shell morphology of the PS–NIPa particles, where the dark spherical area presents the PS core and the light corona around the core shows the cross-linked PNIPa shell. It is worth noting that the shell of PNIPa has a quite regular spherical shape, which is different from the morphology of PS–NIPa particles prepared by the conventional method (see the cryo-TEM images in Fig. 2) [19,57]. Moreover, as shown in Fig. 4, the diameter of the entire core–shell particles measured from the cryo-TEM images is in good agreement with data measured by DLS. The decrease of the thickness of the PNIPa shell with the increase of the cross-linker content in the system is due to the higher cross-linking density of the PNIPa network. This indicates that by changing the cross-linker content in the photo-polymerization procedure it is possible to control the cross-linking density of the shell of PNIPa networks.

Evidently, compared with conventional emulsion polymerization, photo-emulsion polymerization leads to a more homogeneous cross-linked PNIPa shell. Also, the shells are tightly

bound to the cores. This is to be expected as the shell results from a “grafting-from” process, that is, from radicals tightly bound to the surface of the core particles.

3. Characterization

Understanding the phase behaviour of microgel particles is one of the central points for the application of such systems. Light scattering is one of the most common techniques used for structural analysis of microgel particles. Both dynamic light scattering (DLS) and static light scattering (SLS) have been used extensively and remain the standard techniques for particle characterization. There have been many investigations on microgels using DLS or SLS data [68–75]. Pelton et al. [76] have first combined the DLS and electrophoretic mobility data as a function of temperature to characterize PNIPa microgels. Wu [77] has employed DLS to compare the temperature sensitivity of PNIPa microgels to linear PNIPa. They found that the LCST of the PNIPa microgels is slightly lower and the transition is sharper than the one of linear PNIPa. Moreover, other techniques have also allowed for great insight into the structure of microgels. NMR or pulsed-gradient spin echo (PGSE) NMR spectroscopy has been used to investigate the structure of microgels in recent years [78–82]. Pichot et al. [83] investigated the heterogeneous structure inside microgel particles by NMR spectroscopy. Corresponding to the concentration gradients of the cross-linker, they found that the internal particle structure is less cross-linked when going from the core to the shell. Up to now, small-angle neutron scattering (SANS) and small-angle X-ray scattering (SAXS) were often used to study the phase behaviour of microgel particles [27,51,73,84–86] as well. Some time ago a detail review [35] on the investigation of the phase behaviour of the core–shell type microgels by

DLS, SANS, SAXS and rheometric methods was presented. The results revealed that the particles have a well-defined core–shell structure. In particular, the analysis of SANS data performed at elevated temperatures (40 °C) demonstrated unambiguously that the shell is rather compact, that is, the outer radius of the particles is well-defined. Moreover, the SAXS data taken at higher scattering angles showed that the network of the shell exhibits the density fluctuations expected for a swollen network.

Electron microscopic and optical techniques as well as atomic force microscopy (AFM) can be employed easily to investigate the particle morphology. However, microgel particles are usually employed in their wet solvated state. Thus, an in situ characterization of these particles under such conditions by microscopic techniques presents a new challenge. Fujii et al. [87] have described the direct, real space characterization of swollen pH-responsive microgel particles in aqueous solution using scanning transmission X-ray microscopy (STXM). Combining STXM with near-edge X-ray absorption fine structure spectroscopy (NEXAFS), it is possible to provide images of submicrometer-sized swollen microgel particles and to simultaneously determine their chemical state in situ. More recently, we have reported a first study of transition behaviour of thermosensitive core–shell particles by cryo-TEM [57]. Fig. 5 shows the cryo-TEM images for the core–shell microgel particles quenched from room temperature and from 45 °C, respectively. This experiment is more difficult because vitrification must be much faster than the relaxation time characterizing the shrinking kinetics of the particles. From Fig. 5, it can be clearly observed that the thermosensitive shell of the particles is considerably shrunken when the sample was quenched from 45 °C. Moreover, the shell has been compacted by this shrinking process and provides a tight envelope of the

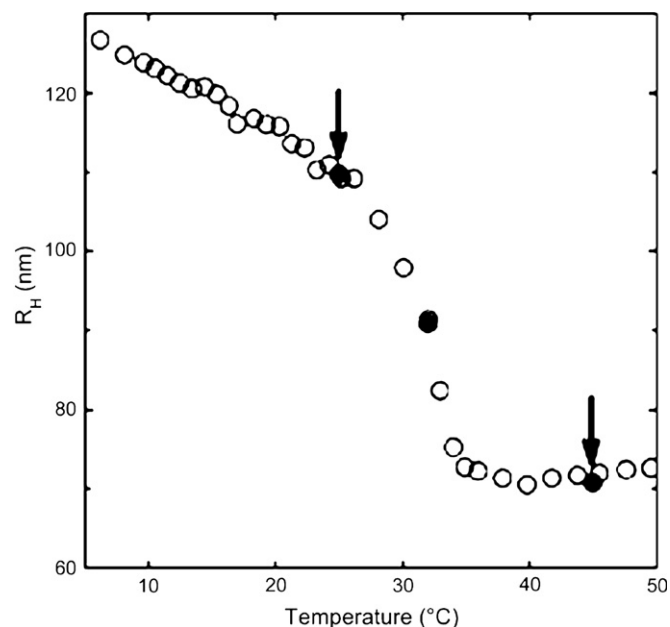


Fig. 6. Hydrodynamic radius of the particles, as measured by dynamic light scattering (90° scattering angle) as the function of temperature. Arrows indicate the temperatures at which the cryo-TEM measurements have been made (Ref. [57]).

core. This also agrees well with the results deduced from SANS measurements [27].

Fig. 6 shows the dependence of the hydrodynamic radius, R_h , as the function of temperature, calculated from DLS data. Comparing the cryo-TEM data to the data taken from DLS measurements, we found that the overall radius of the particles from these images is in good agreement with the hydrodynamic radius measured at corresponding temperatures

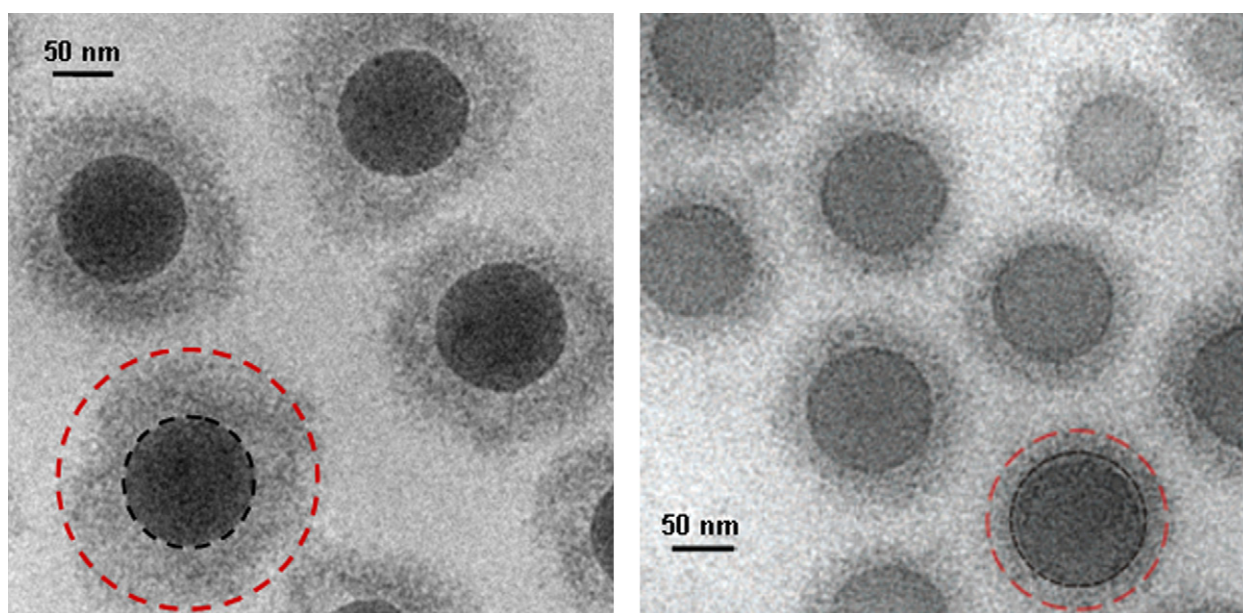


Fig. 5. Cryo-TEM images of PS–PNIPa core–shell particles. The sample was kept at 23 °C (left) and 45 °C (right) before vitrification (Ref. [57]). The circle around the core marks the core radius determined by dynamic light scattering (DLS) in solution. The circle around the entire particle gives the hydrodynamic radius R_h of the core–shell particles as determined by DLS.

(dashed circle). This indicates that cryo-TEM is a good method to describe the volume transition of thermosensitive core–shell particles.

4. Applications

In the following we discuss applications of “smart” microgel particles. Microgels may have several important advantages over other systems, namely, stability, ease of synthesis, good control over particle size, and easy functionalization providing stimulus-responsive behaviour (e.g. change in volume in response to a change in pH, ionic strength or temperature). It becomes clear that this kind of materials holds great promise for nanotechnology. A recent review given by Nayak and Lyon [1] indicated that studies of the detailed structure–function relationships in hydrogel nanoparticles are now leading to the design of applications-oriented nanomaterials.

Here, we will mainly discuss the application of such kind of microgels as carrier systems for the deposition of metal nanoparticles. Antonietti et al. [88,89] were the first to employ microgels as “exotemplates” for the preparation of metal nanoparticles. Recently, Kumacheva et al. [90,91] introduced polymer microgels as carrier systems for nanoparticles. They showed that semiconductors, metal, and magnetic NPs with predetermined size, polydispersity, optical and magnetic properties can be successfully synthesized using polymer microgels as a template, which will have promising applications in catalysis, biolabeling, chemical and biological separation. Biffis et al. [17,18,92] have studied the application of microgel-stabilized metal nanoclusters as catalysts for different reactions and confirmed the enhanced catalytic activity of Pd nanoclusters in Heck reaction of activated aryl bromides, which is attributed to the smaller size of the metal nanoclusters. Suzuki and Kawaguchi [93,94] have reported the novel thermosensitive hybrid core–shell particles via in situ Au or Ag/Au nanoparticle formation using thermosensitive core–shell particles as a template. They found that the color of the hybrid microgels originated from interparticle interactions of nanoparticles changes according to the swelling/deswelling property of the thermosensitive microgel.

Recently, we have successfully used thermosensitive core–shell microgel particles as a template for the deposition of metal nanoparticles (Ag, Au and Pd) [19,20,95]. Fig. 7 displays cryo-TEM images of microgel particles embedded with different metal nanoparticles. From Fig. 7, the dark spherical area indicates the PS core whereas the light corona around the dark core represents the PNIPA shell of the particles. The metal nanoparticles are seen as the small black dots. It is evident that most of the metal nanoparticles are homogeneously immobilized inside the PNIPA networks affixed to the surface of the core particles. Comparing these images in Fig. 7, it is obvious to see that the size of metal nanoparticles is different: Ag nanoparticles (8.5 ± 1.5 nm) are larger than Au (2.0 ± 0.5 nm) and Pd (3.8 ± 0.6 nm) nanoparticles. This may be due to the difference of the complexation of the metal ions with the functional groups of the microgels. However, further investigations by dynamic light

scattering measurements of composite particles indicated that the original thermosensitive properties of the PNIPA network are not suppressed by the incorporation of metal particles into the network. The metal nanoparticles do not alter the volume transition within the network. In addition, it is interesting to note that the surface plasmon absorption band of the silver nanoparticles is shifted to higher wavelengths with temperature, which is traced back to the varying distance of the nanoparticles caused by the swelling and the shrinking of the shell [20]. A similar behaviour has also been observed by Suzuki and Kawaguchi [94].

Recently, we demonstrated that such thermosensitive core–shell particles could act as a smart “nanoreactor” for the metal nanoparticles [19,20]. They allow us to modulate the catalytic activity of nanoparticles by a thermodynamic transition that takes place within the carrier system. The principle is shown in Fig. 8: metallic nanoparticles embedded in such a network are fully accessible by the reactants at low temperature. Above the transition, however, the marked shrinking of the network should be followed by a concomitant slowing down of the diffusion of the reactants within the network. Thus the rate of reactions catalyzed by the nanoparticles should be slowed down considerably. In this way, the network could act as a “nanoreactor” that can be opened or closed to a certain extent.

The catalytic activity was investigated by monitoring photometrically the reduction of 4-nitrophenol by an excess of NaBH_4 in the presence of the metal nanocomposite particles [96–98]. Fig. 9 gives a typical curve for the influence of the temperature on the rate constant k_{app} of the catalytic reaction, which does not follow a typical Arrhenius-type dependence on temperature [20]. When the reaction temperature is low, the PNIPA network is swollen. In this case, metal nanoparticles, which have been embedded in the network can be accessed by the reactants of the catalytic reduction. So the rate constant k_{app} will exhibit a linear relation of $\ln k_{\text{app}}$ with T^{-1} . However, when the temperature is further increasing, the PNIPA network shrinks markedly, which is followed by a concomitant slowing down of the diffusion of reactants within the network. This in turn will lower the rate of reaction catalyzed by the metal nanoparticles. It is obvious that the increase of k_{app} by the raise of temperature is overcompensated by the diffusional barrier. Hence, the reaction rate must reach its minimum at the transition temperature. If the increase of temperature continues, the PNIPA network will not shrink anymore and the density within the network stays constant. Now the strong increase of k_{app} with T will be predominant and the reaction rate will rise again. This demonstrates that the volume transition within a thermosensitive network can be used as a switch. Fig. 9 shows that the catalytic activity of the metallic nanoparticles can be tuned down by more than one order of magnitude.

5. Flow behaviour: towards “smart” fluids

All applications discussed so far require dilute suspensions of the particles, which thus act more or less as individual systems. However, some years ago, Richtering and co-workers [99] demonstrated that the viscoelastic behaviour of

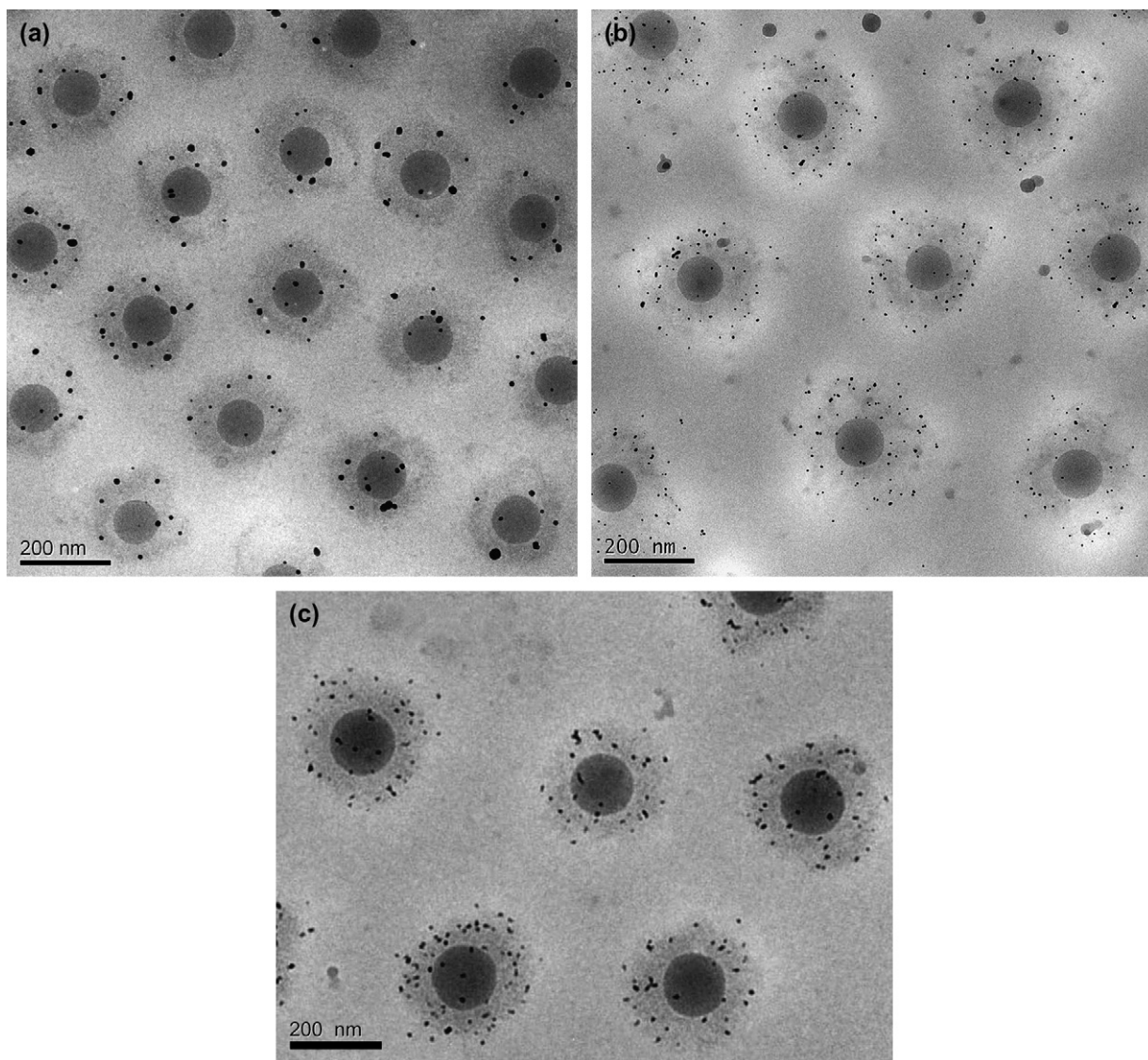


Fig. 7. Cryo-TEM images of microgel particles embedded with different metal nanoparticles: (a) with Ag, (b) with Au, and (c) with Pd nanoparticles.

concentrated suspensions of thermosensitive core–shell particles can be easily tuned by the temperature of the system: at elevated temperatures, the particles are shrunken and their

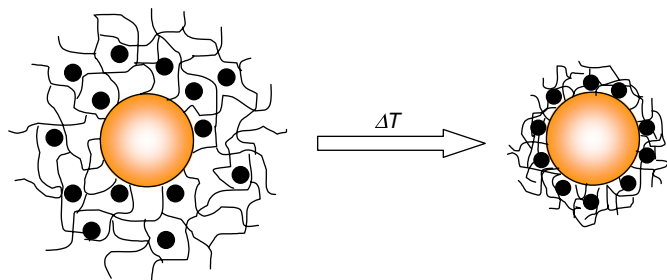


Fig. 8. Schematic representation of composite particles consisting of thermosensitive core–shell particles in which metallic nanoparticles are embedded. The composite particles are suspended in water, which swell the thermosensitive network attached to the surface of the core particles. In this state the reagents can diffuse freely to the nanoparticles which act as catalysts. At higher temperatures ($T > 32\text{ }^{\circ}\text{C}$) the network shrinks and the catalytic activity of the nanoparticles is strongly diminished in this state.

effective volume fraction is low. Hence, the mutual interaction of the particles is small and the viscosity of the suspension is hardly above the one of the suspending medium water. If, however, the temperature is lowered, the thermosensitive shells of the particles will swell through the uptake of water. This in turn will increase the effective volume fraction of the particles considerably. In other words, the swollen particles will begin to interact more strongly and finally touch each other. This will lead to an increase of the viscosity by orders of magnitude and the onset of viscoelastic behaviour.

Recently, it has been shown that the viscoelastic behaviour of concentrated suspensions of spherical particles can be modelled in terms of the mode-coupling theory [100,101]. Applied to the thermosensitive particles under consideration here, mode-coupling theory has met with gratifying success, inasmuch as this theory describes all features related to the observed viscoelastic behaviour in a quantitative manner [102]. Now one may speculate on how the interesting properties of the metal particle composite may be combined with the

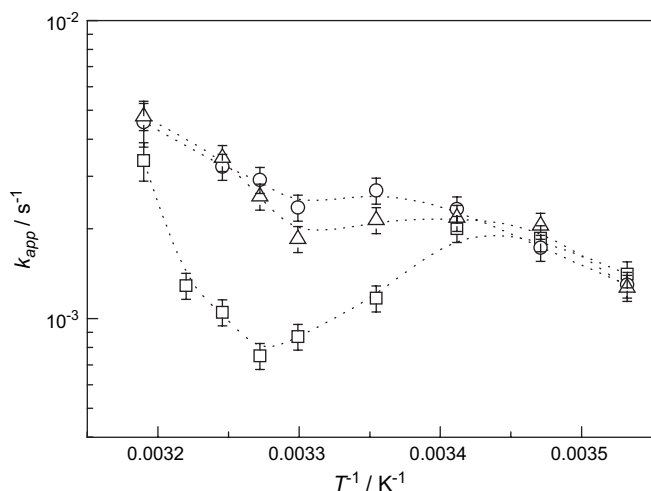


Fig. 9. Arrhenius plot of the reaction rate $k(T)$ measured in presence of PS–NIPA–Ag composite particles at different temperatures. Quadrangles: KPS1–Ag (2.5 mol% BIS); triangles: KPS2–Ag (5 mol% BIS); and circles: KPS3–Ag (10 mol% BIS). The concentrations of the reactants are: composite particles: $S = 0.042 \text{ m}^2/\text{l}$; [4-nitrophenol] = 0.1 mmol/l; $[\text{NaBH}_4] = 10 \text{ mmol/l}$. The broken lines are guidelines for the eye (Ref. [20]).

tunable viscoelasticity which these systems exhibit at sufficiently high concentrations. Here one may envision magnetofluids or fluids with catalytic properties that react on external stimuli. Hence, in this way the macroscopic viscoelastic behaviour as well as the microscopic properties e.g. related to catalysis can be tuned at once. Investigations along this line are under way by now.

6. Conclusion

In this review we have discussed recent work on the preparation and characterization of the thermosensitive core–shell microgel particles and their applications as catalyst. In particular, a novel synthetic method, photo-emulsion polymerization, has been described for the preparation of monodisperse, thermosensitive core–shell particles. Cryogenic transmission electron microscopic (cryo-TEM) images indicate the core–shell morphology of the microgel particles. An increase in temperature leads to the marked shrinking of the thermosensitive PNIPA shell, which was measured by dynamic light scattering. This has been demonstrated for the first time by cryo-TEM. Such kind of microgels can be used as “nanoreactors” for the immobilization of metal nanoparticles. The metal nanocomposite particles exhibit “smart” catalytic behaviour as the catalytic activity of nanoparticles can be modulated by a thermodynamic transition taken place within the carrier system.

Acknowledgment

The authors thank the Deutsche Forschungsgemeinschaft, SFB 481, Bayreuth, and Schwerpunktprogramm “Hydrogele” (SPP1259/1), the BASF-AG, and Fonds der Chemischen Industrie for financial support.

References

- [1] Nayak S, Lyon LA. *Angew Chem Int Ed* 2005;44:7686–708.
- [2] Pelton R. *Adv Colloid Interface Sci* 2000;85:1–33.
- [3] Hoshino F, Fugimoto T, Kawaguchi H, Ohtsuka Y. *Polym J* 1987;19:241–7.
- [4] Jones CD, Lyon LA. *Macromolecules* 2000;33:8301–6.
- [5] Dupin D, Fujii S, Armes SP, Reeve P, Baxter SM. *Langmuir* 2006;22:3381–7.
- [6] Nayak S, Lyon LA. *Chem Mater* 2004;16:2623–7.
- [7] Mcphee W, Tam KC, Pelton R. *J Colloid Interface Sci* 1993;156:24–30.
- [8] Zrinyi M. *Colloid Polym Sci* 2000;278:98–103.
- [9] Das M, Mardiyani S, Chan WCW, Kumacheva E. *Adv Mater* 2006;18:80–3.
- [10] Nayak S, Lee H, Chmielewski J, Lyon LA. *J Am Chem Soc* 2004;126:10258–9.
- [11] Soppimath KS, Tan DCW, Yang Y. *Adv Mater* 2005;17:318–23.
- [12] Hu Z, Chen Y, Wang C, Zheng Y, Li Y. *Nature* 1998;393:149–52.
- [13] Kawaguchi H, Fujimoto K. *Bioseparation* 1999;7:253–8.
- [14] Sahiner N, Godbey WT, Mcpherson GL, John VT. *Colloid Polym Sci* 2006;284:1121–9.
- [15] Bouillot P, Vincent B. *Colloid Polym Sci* 2000;278:74–9.
- [16] Bergbreiter DE, Liu YS, Osburn PL. *J Am Chem Soc* 1998;120:4250–1.
- [17] Biffis A, Orlandi N, Corain B. *Adv Mater* 2003;15:1551–5.
- [18] Biffis A, Minati L. *J Catal* 2005;236:405–9.
- [19] Lu Y, Mei Y, Drechsler M, Ballauff M. *Angew Chem Int Ed* 2006;45:813–6.
- [20] Lu Y, Mei Y, Drechsler M, Ballauff M. *J Phys Chem B* 2006;110:3930–7.
- [21] Heskins M, Guillet JE. *J Macromol Sci Chem A* 1968;2:1441–55.
- [22] Schild HG. *Prog Polym Sci* 1992;17:163–249.
- [23] Wu C, Wang X. *Phys Rev Lett* 1998;80:4092–4.
- [24] Hellweg T, Dewhurst CD, Eimer W, Kratz K. *Langmuir* 2004;20:4330–5.
- [25] Cho CS, Cheon JB, Jeong YL, Kim IS, Kim SH, Akaike T. *Macromol Rapid Commun* 1997;18:361.
- [26] Jones CD, Lyon LA. *Langmuir* 2003;19:4544–7.
- [27] Dingenouts N, Seelenmeyer S, Deike I, Rosenfeldt S, Ballauff M, Lindner P, et al. *Phys Chem Chem Phys* 2001;3:1169–74.
- [28] Pelton RH, Chibante P. *Colloids Surf* 1986;20:247–56.
- [29] Snowden MJ, Vincent B. *J Chem Soc Chem Commun* 1992;16:1103–5.
- [30] Kawaguchi H, Fujimoto K, Mizuhara Y. *Colloid Polym Sci* 1992;270:53–7.
- [31] Wu C, Zhou S. *J Polym Sci Part B Polym Phys* 1996;34:1597–604.
- [32] Zhou G, Elaissari A, Delair Th, Pichot C. *Colloid Polym Sci* 1998;276:1131–9.
- [33] Pichot C, Duracher D, Elaissari A, Mallet F. *Polym Prepr Am Chem Soc Div Polym Chem* 2000;41:1026–7.
- [34] Pelton RH. *J Polym Sci* 1988;26:9–18.
- [35] Ballauff M. *Macromol Chem Phys* 2003;204:220–34.
- [36] Hellweg T, Dewhurst CD, Bruckner E, Kratz K, Eimer W. *Colloid Polym Sci* 2000;278:972–8.
- [37] Nayak S, Gan D, Serpe MJ, Lyon LA. *Small* 2005;1:416–21.
- [38] Berndt I, Popescu C, Wortmann FJ, Richtering W. *Angew Chem Int Ed* 2006;45:1081–5.
- [39] Berndt I, Pedersen JS, Richtering W. *Angew Chem Int Ed* 2006;45:1737–41.
- [40] Ngai T, Behrens SH, Auweter H. *Chem Commun* 2005;3:331–3.
- [41] Hoare T, Pelton R. *Langmuir* 2004;20:2123–33.
- [42] Hoare T, Pelton R. *Macromolecules* 2004;37:2544–50.
- [43] Hoare T, Pelton R. *Polymer* 2005;46:1139–50.
- [44] Zhou S, Chu B. *J Phys Chem B* 1998;102:1364–71.
- [45] Leung MF, Zhu J, Harris FW, Li P. *Macromol Symp* 2005;226:177–85.
- [46] Nizri G, Magdassi S, Schmidt J, Talmon Y. *Langmuir* 2004;20:4380–5.
- [47] Li Z, Kesselman E, Talmon Y, Hillmyer MA, Lodge TP. *Science* 2004;306:98–101.

- [48] Makino K, Yamamoto S, Fujimoto K, Kawaguchi H, Oshima H. *J Colloid Interface Sci* 1994;166:251–8.
- [49] Okubo M, Ahmad H. *Colloid Polym Sci* 1996;274:112–6.
- [50] Kim JH, Ballauff M. *Colloid Polym Sci* 1999;277:1210–8.
- [51] Dingenouts N, Norhausen Ch, Ballauff M. *Macromolecules* 1998;31:8912–7.
- [52] Castanheira EMS, Martinho JMG, Duracher D, Charreyre MT, Elaissari A, Pichot C. *Langmuir* 1999;15:6712–7.
- [53] Santos AM, Elaissari A, Martinho JMG, Pichot C. *Polymer* 2005;46:1181–8.
- [54] Prazeres TJV, Fedorov A, Martinho JMG. *J Phys Chem B* 2004;108:9032–41.
- [55] Xiao XC, Chu LY, Chen WM, Wang S, Li Y. *Adv Funct Mater* 2003;13:847–52.
- [56] Wittemann A, Drechsler M, Talmon Y, Ballauff M. *J Am Chem Soc* 2005;127:9688–9.
- [57] Crassous J, Drechsler Y, Talmon Y, Ballauff M. *Langmuir* 2006;22:2403–6.
- [58] Seelenmeyer S, Deike I, Rosenfeldt S, Norhausen Ch, Ballauff M, Narayanan I. *J Chem Phys* 2001;114:10471–8.
- [59] Wu X, Pelton RH, Hamielec AE, Woods DR, McPhee W. *Colloid Polym Sci* 1994;272:467–77.
- [60] Kuckling D, Vo CD, Wohlrab S. *Langmuir* 2002;18:4263–9.
- [61] Kuckling D, Vo CD, Adler HJP, Voelkel A, Coelfen H. *Macromolecules* 2006;39:1585–90.
- [62] Qiao X, Zhang Z, Yao S. *J Photochem Photobiol A Chem* 2006;177:191–6.
- [63] Lu Y, Wittemann A, Drechsler M, Ballauff M. *Macromol Rapid Commun* 2006;27:1137–41.
- [64] Guo X, Weiss A, Ballauff M. *Macromolecules* 1999;32:6043–6.
- [65] Guo X, Ballauff M. *Langmuir* 2000;16:8719–26.
- [66] Sharma G, Ballauff M. *Macromol Rapid Commun* 2004;25:547–52.
- [67] Lu Y, Mei Y, Walker R, Ballauff M, Drechsler M. *Polymer* 2006;47:4985–95.
- [68] Saunders BR, Vincent B. *Adv Colloid Interface Sci* 1999;80:1–25.
- [69] Wu C, Zhou S. *Macromolecules* 1997;30:574–6.
- [70] Wu C, Zhou S. *J Macromol Sci Phys* 1997;36:345–55.
- [71] Yi YD, Oh KS, Bae YC. *Polymer* 1997;38:3471–6.
- [72] Varga I, Gilanyi T, Meszaros R, Filipcsei G, Zrinyi M. *J Phys Chem B* 2001;105:9071–6.
- [73] Kratz K, Hellweg T, Eimer W. *Polymer* 2001;42:6631–9.
- [74] Ma X, Xi J, Huang X, Zhao X, Tang X. *Mater Lett* 2004;58:3400–4.
- [75] Boyko V, Pich A, Lu Y, Richter S, Arndt KF, Adler HJ. *Polymer* 2003;44:7821–7.
- [76] Pelton RH, Pelton HM, Morphis A, Rowell RL. *Langmuir* 1989;5:816–8.
- [77] Wu C. *Polymer* 1998;39:4609–19.
- [78] Sierra-Martin B, Romero-Cano MS, Terence Cosgrove, Vincent B, Fernandez-Barbero A. *Colloids Surf A* 2005;270:296–300.
- [79] Griffiths PC, Stilbs P, Chowdhry BZ, Snowden MJ. *Colloid Polym Sci* 1995;273:405–11.
- [80] Andersson M, Hietala S, Tenhu H, Maunu SL. *Colloid Polym Sci* 2006;284:1255–63.
- [81] Zhu PW, Napper DH. *Colloids Surf A* 1996;113:145–53.
- [82] Schönhoff M, Larsson A, Welzel PB, Kuckling D. *J Phys Chem B* 2002;106:7800–8.
- [83] Guillermo A, Addad JPC, Bazile JP, Duracher D, Elaissari A, Pichot C. *J Polym Sci Part B Polym Phys* 2000;38:889–98.
- [84] Seelenmeyer S, Deike I, Dingenouts N, Rosenfeldt S, Norhausen Ch, Ballauff M, et al. *J Appl Crystallogr* 2000;33:574–6.
- [85] Koh AYC, Saunders BR. *Langmuir* 2005;21:6734–41.
- [86] Berndt I, Pedersen JS, Lindner P, Richtering W. *Langmuir* 2006;22:459–68.
- [87] Fujii S, Armes SP, Araki T, Ade H. *J Am Chem Soc* 2005;127:16808–9.
- [88] Antonietti M, Groehn F, Hartmann J, Bronstein L. *Angew Chem Int Ed* 1997;36:2080–3.
- [89] Whilton NT, Berton B, Bronstein L, Henze H, Antonietti M. *Adv Mater* 1999;11:1014–8.
- [90] Zhang J, Xu S, Kumacheva E. *J Am Chem Soc* 2004;126:7908–14.
- [91] Zhang J, Xu S, Kumacheva E. *Adv Mater* 2005;17:2336–40.
- [92] Biffis A, Sperotto E. *Langmuir* 2003;19:9548–50.
- [93] Suzuki D, Kawaguchi H. *Langmuir* 2005;21:12016–24.
- [94] Suzuki D, Kawaguchi H. *Langmuir* 2006;22:3818–22.
- [95] Mei Y, Lu Y, Polzer F, Ballauff M, Drechsler M. *Chem Mater* 2007;19(5):1062–9.
- [96] Pich A, Karak A, Lu Y, Boyko V, Adler HJP. *Macromol Rapid Commun* 2006;27:344–50.
- [97] Pradhan N, Pal A, Pal T. *Colloids Surf A* 2002;196:247–57.
- [98] Antipov AA, Sukhorukov GB, Fedutik YA, Hartmann J, Giersig M, Mochwald H. *Langmuir* 2002;18:6687–93.
- [99] Senff H, Richtering W, Norhausen Ch, Weiss A, Ballauff M. *Langmuir* 1999;15:102–6.
- [100] Fuchs M, Ballauff M. *J Chem Phys* 2005;122:094707/1–094707/6.
- [101] Fuchs M, Ballauff M. *Colloid Surf A* 2005;270–271:232–8.
- [102] Crassous JJ, Siebenbürger M, Ballauff M, Drechsler M, Henrich O, Fuchs M. *J Chem Phys* 2006;125:204906/1–204906/11.



Matthias Ballauff studied chemistry at the University of Mainz, where he received his degree in 1977 in the group of Professor Dr. B.A. Wolf. In 1981, he received his doctorate working in the same group at the Institute of Physical Chemistry. From 1981 to 1983, Matthias Ballauff was a post-doc in Professor P.J. Flory's group at Stanford University, where he studied liquid crystalline polymers and defined liquid crystalline model oligomers. He then worked with Professor Dr. G. Wegner and Professor Dr. E.W. Fischer at the Max Planck Institute for Polymer Research in Mainz. After his habilitation at the University of Mainz in

1989, Matthias Ballauff became Professor in the Faculty of Chemistry at the University of Karlsruhe. Since 2003, Matthias Ballauff is professor for physical chemistry (Lehrstuhl Physikalische Chemie I) in the University of Bayreuth. Professor Ballauff was a member of the DFG committee for areas of special research and is a member of the board of the journal *Colloid & Polymer Science*, and a member of the Executive Advisory Board for the *Macromolecular Journals*.



Yan Lu was born in Wuxi, China. She received her Masters degree in Material Science at Donghua University (formerly China Textile University) in 2001. In 2005, she received her PhD with *summa cum laude* under the supervision of Prof. Dr. H.-J.P. Adler at the Institute of Macromolecular Chemistry and Textile Chemistry in Dresden University of Technology, Germany. Since 2005, she works as post-doctor in Prof. Dr. M. Ballauff's group at the Department of Physical Chemistry I, University of Bayreuth. She was awarded "API-Prize" for the best dissertation in 2005 by the German Chemical Society (GDCh) Division of Coatings and Pig-

ments. Her research interests cover synthesis and characterization of polymer colloids, including polyelectrolyte brushes and microgels, and synthesis of metal nanocomposite particles.